catalysts

MDPI

Article

The Effect of Sr Addition in Cu- and Fe-Modified CeO_2 and ZrO_2 Soot Combustion Catalysts

Verónica Rico-Pérez, Eleonora Aneggi * and Alessandro Trovarelli

Dipartimento Politecnico di Ingegneria e Architettura, Università degli Studi di Udine, via Cotonificio 108, 33100 Udine, Italy; veronica.rico@uniud.it (V.R.-P.); trovarelli@uniud.it (A.T.)

* Correspondence: eleonora.aneggi@uniud.it; Tel.: +39-0432-558-830

Academic Editors: Enrique Rodríguez-Castellón, Agustín Bueno-López and Elisa Moretti

Received: 27 December 2016; Accepted: 11 January 2017; Published: 17 January 2017

Abstract: This study investigates the activity of transition and alkaline-earth metal-doped catalysts supported on ceria or zirconia for the NO_x-assisted oxidation of diesel particulate. A series of Cu- and Fe-impregnated catalysts over CeO_2 and ZrO_2 supports were prepared by incipient wetness impregnation and characterized by BET, X-ray diffraction (XRD), and temperature-programmed reduction (TPR) experiments while their catalytic activity was investigated in NO_x-assisted reaction by means of temperature programmed oxidation experiments (TPO). Higher activity was achieved by copper modified catalysts; the addition of Sr positively affected the performance of the materials, suggesting a synergic effect between transition metals and alkaline-earth metal. The role of copper is correlated to the oxidation of NO to NO_2, while strontium seems to be mainly involved in the storage of NO_x species.

Keywords: ceria; zirconia; soot oxidation; CuO; Fe_2O_3; strontium

1. Introduction

Diesel engines have increased popularity in recent years due to their higher efficiency compared to gasoline engines. Particulate matter (PM), or soot particles, are formed as undesired by-products of the combustion process, being one of the main pollutants emitted by diesel engines, together with NO_x, CO, and unburned hydrocarbons [1]. Particulate, which is composed of aggregated carbonaceous soot and soluble organic fraction (SOF) of condensed hydrocarbons on soot, is a potential carcinogen and contributes to respiratory issues [2,3]. Regulations on diesel exhaust emissions have become always more and more stringent and this has stimulated researchers to develop emission-reduction technologies. Among the various methodologies developed, the diesel particulate filter (DPF) loaded with a soot oxidation catalyst is one of the most efficient devices to reduce soot emissions [4–7].

Two different strategies could be adopted for catalytic regeneration of the filter: one approach is to increase the contact points between the soot particles and the catalysts (i.e., by using fuel-borne catalyst additives or molten salt catalysts that can "wet" the soot surface and, therefore, decrease the oxidation temperature [8–10]). Another strategy is to use an oxidation catalyst that can promote the formation of mobile compounds (i.e., active oxygen species, or NO_2 from NO) which then act as the true oxidant for soot in a more active and efficient way compared to O_2. An example is the oxidation of soot over Pt-based catalysts where Pt promotes NO oxidation to NO_2, and the latter oxidizes carbon. Subsequently, the nitrogen dioxide will convert soot into CO and CO_2 and back to NO, which can participate in the next soot oxidation event [11].

Several catalytic materials were developed in the last decade [12] and the most promising are based on transition metals (Ag, Co, Cu, Mn, Fe) [13–27], ceria-doped materials [28–36], alkaline or alkaline-earth metals [37–41], and perovskites [42,43]. The redox capacity of transition metals, cycling between more oxidation states, can efficiently enhanced soot oxidation activity. The mechanism of the reaction is based on the formation of "active oxygen" species that can easily react with soot,

decreasing the temperature of combustion. Moreover, their redox cycle can also successfully oxidize NO to NO_2, thus activating the NO_x-assisted reaction as an alternative soot oxidation route, where nitrogen dioxide is directly involved in soot combustion due to its more powerful oxidation capacity. Among transition metals, Fe and Cu have often been employed as dopants/promoters of soot oxidation catalysts supported on metal oxides with different properties, such as alumina, titania, zirconia, and ceria [16,19,22,44–47]. The mechanism path commonly proposed for Cu- and Fe-based materials is correlated to the presence of metal oxide particles and their capability to be cyclically reduced and then reoxidized by O_2 gas phase or lattice oxygen from the support [45,48,49].

Cerium and zirconium oxide are widely used as supports in several catalytic reactions. Zirconia is a "non-reducible" oxide (in the typical reaction conditions used for soot oxidation) that displays useful physical and chemical properties, i.e., chemical stability, low thermal conductivity, and high corrosion resistance. On the other hand, ceria-based materials are successfully used in several catalytic applications due to their high availability of surface oxygen and high surface reducibility [28,29]. It is believed that the activity of ceria on soot combustion is due to its redox activity and its ability to deliver oxygen from the lattice to the carbon particles [50].

The introduction of alkali or alkaline-earth metals, on catalytic formulations, results in an enhanced catalytic activity in soot oxidation [37,40,41]. Alkaline-earth metals can promote soot combustion activity, working either as oxidation catalysts or NO_x storage traps [51–54]. Indeed, on alkaline-earth metal NO_x storage occurs suggesting their use as a promising component in LNT (lean NO_x trap) applications where NO_x is stored during the lean phase and then it is reduced in the rich interval. Recently, a synergic effect by simultaneous doping of CeO_2 by alkaline or alkaline-earth metals (K and Ba) and copper has been reported [54,55]. The lowering of the oxidation temperatures is obtained by the increased NO_x storage capacity brought about by K (or Ba) and Cu.

In light of these considerations, in this study we proposed to combine the potential capacity of copper and iron supported catalysts with the promotional effect of an alkaline metal like strontium. A series of Cu- and Fe-impregnated catalysts over CeO_2 and ZrO_2 supports were prepared and the effect of the presence of Sr in the formulation was investigated. The catalysts have been characterized and their catalytic activity was investigated in NO_x-assisted soot oxidation reaction by means of temperature-programmed oxidation experiments (TPO).

2. Results and Discussion

2.1. Textural and Structural Characterization

Composition and BET surface area of the catalysts are reported in Table 1. Similar BET surface areas have been found for all catalysts (in the range 17–35 m^2/g). The addition of a single component to the support (CeO_2 or ZrO_2) does not affect the surface area that remains almost stable, while a small decrease was observed after addition of the two dopants in the Sr-doped materials. In accordance with the BET results, crystal size values are in the range 13–22 nm.

Table 1. Composition and textural characterization of investigated samples.

Sample	Composition	Surface Area (m^2/g)	Particle Size (nm)
Ce	CeO_2	35	19
CeCu	Cu(5%)/CeO_2	35	13
CeFe	Fe(5%)/CeO_2	30	15
CeSr	Sr(10%)/CeO_2	32	14
CeSrCu	Cu(5%)-Sr(10%)/CeO_2	24	19
CeSrFe	Fe(5%)-Sr(10%)/CeO_2	17	13
Zr	ZrO_2	27	22
ZrCu	Cu(5%)/ZrO_2	32	18
ZrFe	Fe(5%)/ZrO_2	26	18
ZrSr	Sr(10%)/ZrO_2	29	17
ZrSrCu	Cu(5%)-Sr(10%)/ZrO_2	21	18
ZrSrFe	Fe(5%)-Sr(10%)/ZrO_2	22	17

The structural features of all the materials were analysed by powder X-ray diffraction (XRD). Diffraction profiles of ceria-based catalysts (Figure 1A) exhibit reflections characteristic of a pure fluorite phase, while zirconia-based materials show a monoclinic structure (Figure 1B). In ceria-based catalysts, two very weak peaks, characteristic of a CuO phase, were also detected at $2\theta = 35.5°$ and 38.8° for CeCu and CeSrCu samples, which is in agreement with other studies in the literature [20,54]. $SrCO_3$ phase was also detected for Sr impregnated materials (CeSr, CeSrFe, and CeSrCu) and it may occur as a consequence of the exposure of the catalysts to ambient air conditions; indeed, the basic oxides such as the oxides of alkaline-earth elements are readily carbonated when exposed in air [56,57]. No evidence of the presence of Fe_2O_3 or other iron-containing phases was obtained, in accordance with the literature [22,44,58]. XRD features do not indicate formation of any ceria solid solution with copper or iron, suggesting that Fe or Cu are dispersed on the surface. It is known that lower valence ions, such as Fe^{3+} and Cu^{2+}, do not easily dissolve into the ceria lattice using conventional impregnation methods; dissolution, if present, is limited to a small fraction of the overall loading [22,59]. To facilitate formation of solid solution alternative preparation methods are required [60,61]. In zirconia-based samples no evidence for any copper or iron phase was found, while formation of $SrCO_3$ and $SrZrO_3$ phases was observed.

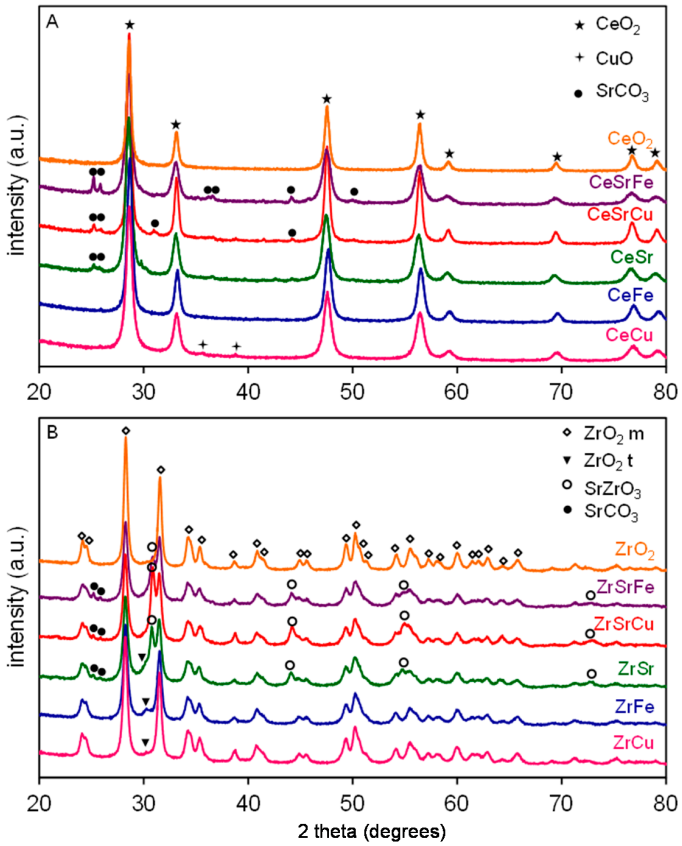

Figure 1. XRD diffraction profiles for (**A**) Ce- and (**B**) Zr-based catalysts.

2.2. Reduction Behaviour

In order to characterize the reduction behaviour of the materials, temperature-programmed reduction experiments with H_2 (H_2-TPR) have been carried out on all samples (Figure 2). Figure 2A shows the temperature programmed reduction profiles of ceria and ceria modified catalysts. The reduction feature of pure ceria is well known and it shows the characteristic bimodal profile with two peaks at low (ca. 525 °C) and high (ca. 840 °C) temperature attributable, respectively, to the reduction of small crystallites and/or surface ceria and to the reduction of bulk and large ceria

crystallites [62]. For pure zirconia, a TPR feature of a typical "non-reducible" support was found (Figure 2B). The reduction profiles of the two supports are affected by the addition of metals.

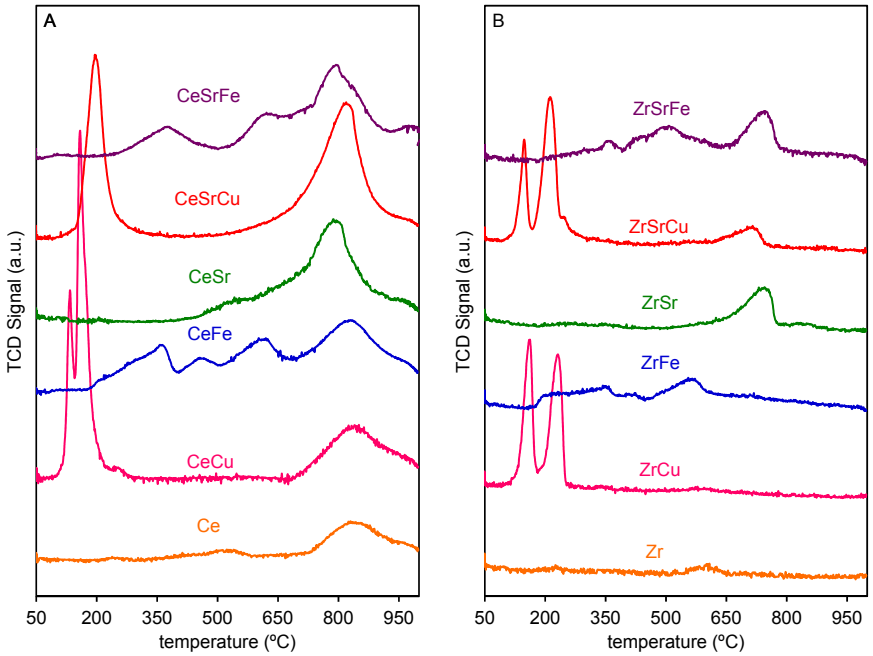

Figure 2. H_2-TPR profiles for (**A**) Ce- and (**B**) Zr-based catalysts.

ZrFe shows two reduction signals that could be ascribed to the existence of free Fe_2O_3 on the support surface. The hydrogen reduction profile for Fe_2O_3 occurs in two steps, with Fe_2O_3 first converting to Fe_3O_4 (with maximum at around 340 °C) and then to Fe (with maximum at ca. 550 °C) [63,64]. In CeFe, reduction of iron species overlap with the reduction features of ceria and four peaks are distinguished: the first one at around 350 °C was related to the reduction of hematite to magnetite state; the second and third peaks at around 450 °C and 600 °C can be attributed to the surface reduction of Ce^{4+} and the reduction of Fe^{2+} to Fe, while the last signal at 825 °C can be associated with the reduction of bulk ceria [65,66].

Materials loaded with Sr evidenced a main peak at around 700–750 °C that could be correlated to the desorption of superficial carbonate species, as confirmed by the analysis of outlet gas composition followed by an online quadrupole mass-spectrometer. For CeSr, the peak overlaps with the bulk reduction feature of ceria.

For the CeSrFe, the H_2-TPR profile undergoes some modifications respect CeFe and only three reduction features are detected due to the merging of the first two signals of CeFe. The low temperature peak (375 °C) is correlated to the reduction of Fe^{3+} to Fe^{2+} and to the reduction of surface Ce^{4+}. The second signal (600 °C), corresponding to the third peak in CeFe, is not affected by the presence of Sr in the formulation. Moreover, the high temperature peak band (790 °C) is due to the overlapping of bulk reduction of ceria and the desorption of carbonate species from the Sr phase.

ZrSrFe is less affected by Sr addition and the TPR profile is the result of the combination of ZrSr and ZrFe features. The first two peaks are due to the iron oxide reduction (as in the ZrFe sample) while the high temperature signal is due to the surface carbonate adsorbed on Sr (as in ZrSr).

The addition of Cu on ceria modifies the redox properties of both species, as a consequence of the CuO-CeO_2 interaction at the oxide interface [59,67–69]. TPR profile of CeCu exhibits three main reduction peaks at 130, 160, and 840 °C. The two low-temperature signals can be assigned to the reduction of CuO_x species and surface Ce^{4+}. It is well known that bulk CuO reduction takes place at around 315–380 °C [20,67,68] while in our material a shift to lower temperature of the CuO_x reduction

features occurs due to metal support interaction. In addition, we can observe that the low reduction signal of ceria at around 525 °C is not present, indicating that the hydrogen spillover process promotes surface ceria reduction at a much lower temperature [67,70]. The quantitative analysis of the TPR profile reveals that a part of Ce^{4+} is reduced at 100–300 °C; the amount of hydrogen consumption in this temperature range (1.10 mmol/g_{cat}) is larger than that required for the complete reduction of CuO_x species (0.79 mmol/g_{cat}), in agreement with other studies [20,70]. The presence of copper can, therefore, promote the reduction of surface ceria at much lower temperatures. The presence of Sr slightly modifies the shape and position of the low temperature signals, and only one peak is visible in CeSrCu, shifted at a slightly higher temperature. The modification of the reduction profile at low temperature can also be associated to a detrimental effect on the reduction properties of the catalyst, confirmed by the decrease of the H_2 consumption at low temperature compared to CeCu (0.83 vs. 1.10 mmol/g_{cat}).

Generally, CuO-CeO_2 materials exhibit more than one reduction peaks correlated to Cu [20,68,70], suggesting the presence of more than one copper oxide species. A great amount of literature data is available for TPR studies of Cu-based catalysts; although shape and position highly depend on the experimental conditions and on the preparation of the catalyst, the shift to lower temperature of the reduction peaks suggests a synergic interaction between CuO and CeO_2. The low temperature peak (typically denoted as peak α) is usually attributed to highly-dispersed CuO species closely interacting with CeO_2 (more easily reduced species), while the higher temperature peak (typically denoted as peak β) is assigned to the overlapping of the reduction of larger CuO particles (still highly dispersed and strongly interacting with the support) and surface Ce^{4+}. Usually a third reduction peak at higher temperature is found in TPR profile of CuO-CeO_2 catalyst (not present in our materials) and is correlated with reduction of segregated crystalline CuO [67,68].

The low temperature region of ZrCu sample is comparable to CeCu, indeed, two peaks at 160 °C and 230 °C due to the reduction of copper species are displayed. The main difference between CeCu and ZrCu is the consumption of H_2 in the low-temperature range, and that, for the latter, corresponds only to the reduction from Cu^{2+} to Cu°, as we can expect for a "non-reducible" support like zirconia (0.70 mmol/g). These peaks are found also in the ZrSrCu sample, where a peak at high temperature (710 °C) due to the contribution of adsorbed strontium carbonate is also detected.

2.3. Catalytic Tests

Figure 3 summarizes the results of soot combustion studies carried out under O_2/N_2 and $NO/O_2/N_2$ atmosphere in terms of peak-top temperature (*T*p). A representative oxidation profile is shown in Figure 4 for the CeSrCu sample.

In O_2 atmosphere (Figure 3A) all of the catalyst formulation are slightly active compared to the oxidation of soot without a catalyst, displaying *T*p in the range 580–595 °C with the exception of CeSr, Zr, and ZrCu, which show temperatures of oxidation higher than 600 °C.

Several studies investigated the promotional effects of copper and iron in soot combustion catalysts under O_2 atmosphere [20,22,45,48]. The mechanism of reaction commonly proposed is correlated to the presence of M_xO_y particles and the ability of the metal to be reduced to $M^{(n-1)+}$ and then reoxidized to M^{n+}, producing active oxygen species that can easily react with soot [45,50].

The addition of NO in the reaction mixture (Figure 3B) causes a decrease in the temperature of combustion for all catalysts (Tp lower than 560 °C). The addition of Cu and Fe results in a beneficial effect on soot combustion compared to bare supports, while the introduction of Sr has a detrimental influence on the performances. The fact that Sr acts as an efficient NO_x trap [52,71,72], with the formation of stable nitrates species, is likely to cause a loss of soot combustion activity, in agreement with previous literature results [15].

With transition metals and Sr containing formulations, the oxidation is shifted at temperatures lower than 500 °C, suggesting a synergic effect of the two components. The best performances are obtained with Cu-Sr combination, with a *T*p of 468 and 482 °C for Zr and Ce sample, respectively, compared to 501 °C and 496 °C for SrFeZr and SrFeCe.

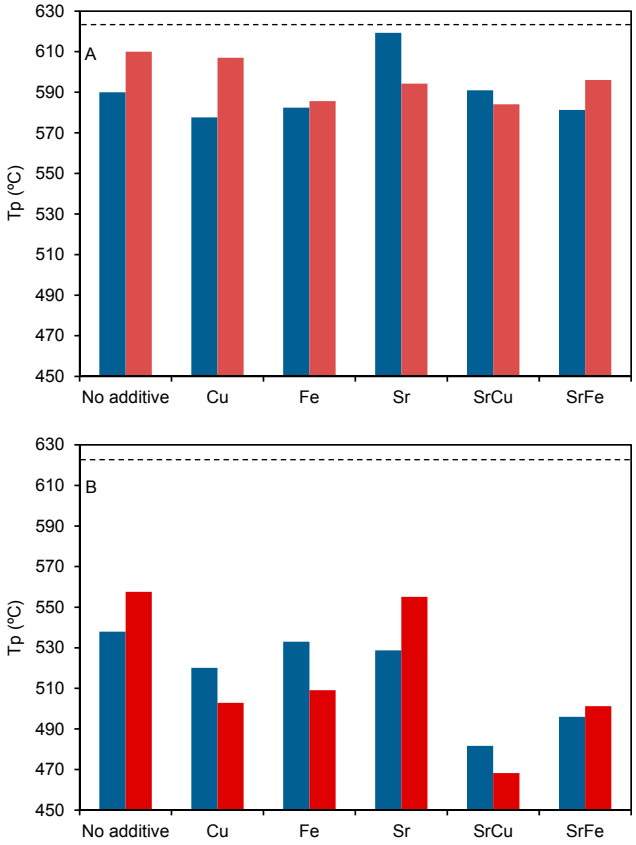

Figure 3. Catalytic activity as *T*p (°C) for soot combustion under loose contact conditions in (**A**) O_2/N_2 and (**B**) $NO/O_2/N_2$ atmosphere for CeO_2 (**blue**)- and ZrO_2 (**red**)-based catalysts. The broken line indicates the soot oxidation temperature for uncatalyzed reactions.

As shown in Figure 4 when soot oxidation is carried out with a mixture of NO/O_2, an enhancement in catalytic combustion was found, compared to the reaction performed under oxygen environment and the reason could be ascribed to two different mechanisms that could take part in a NO/O_2 atmosphere: (i) from one side soot can be oxidized by active oxygen species (O*) that are generated over Cu- or Fe-containing materials, i.e., transition metals exhibit the capability to cycle between two states of oxidation contributing to soot combustion [45,48,49]; (ii) on the other hand, the NO_x-assisted mechanism can improve the catalytic activity forming NO_2, a more oxidant and mobile species [71].

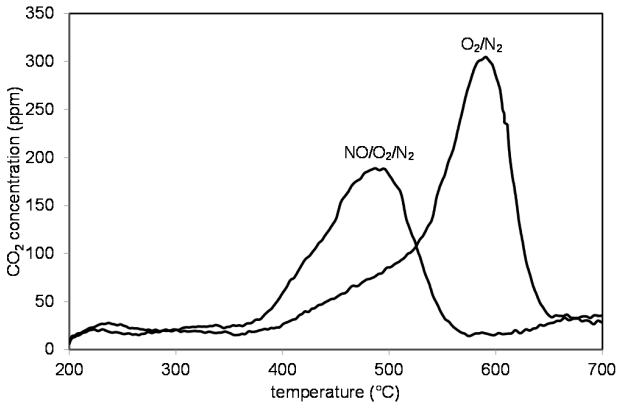

Figure 4. Soot oxidation carried out in a conventional flow reactor by monitoring evolution of CO_2 in O_2/N_2 and $NO/O_2/N_2$ atmosphere for a CeSrCu sample.

In the case of NO_x-assisted reaction it is important that the catalyst can promote the oxidation of NO to NO_2 at low temperature. If NO_2 is formed at temperature lower than that of soot oxidation, it can participate to reaction and offer an alternative route in the combustion of particulate. CeCu is the most active catalyst in NO oxidation as shown in Figure 5, with a Tm lower than 400 °C. All of the other samples containing Cu and Fe exhibit a Tm in the range 425–470 °C, with the exception of pure zirconia, CeSr and ZrSr samples that are only moderately active in NO oxidation (*T*m is higher than 500 °C). In the presence of NO, Cu- and Fe-loaded ceria and zirconia promote soot combustion at lower temperature, showing that catalysts that are more efficient in NO oxidation are more active in soot combustion. This can be clearly seen in Figure 6, where the *T*p vs. Tm temperatures are reported and a correlation between soot combustion (*T*p) and NO oxidation (*T*m) temperatures can be found for both CeO_2- and ZrO_2-based materials.

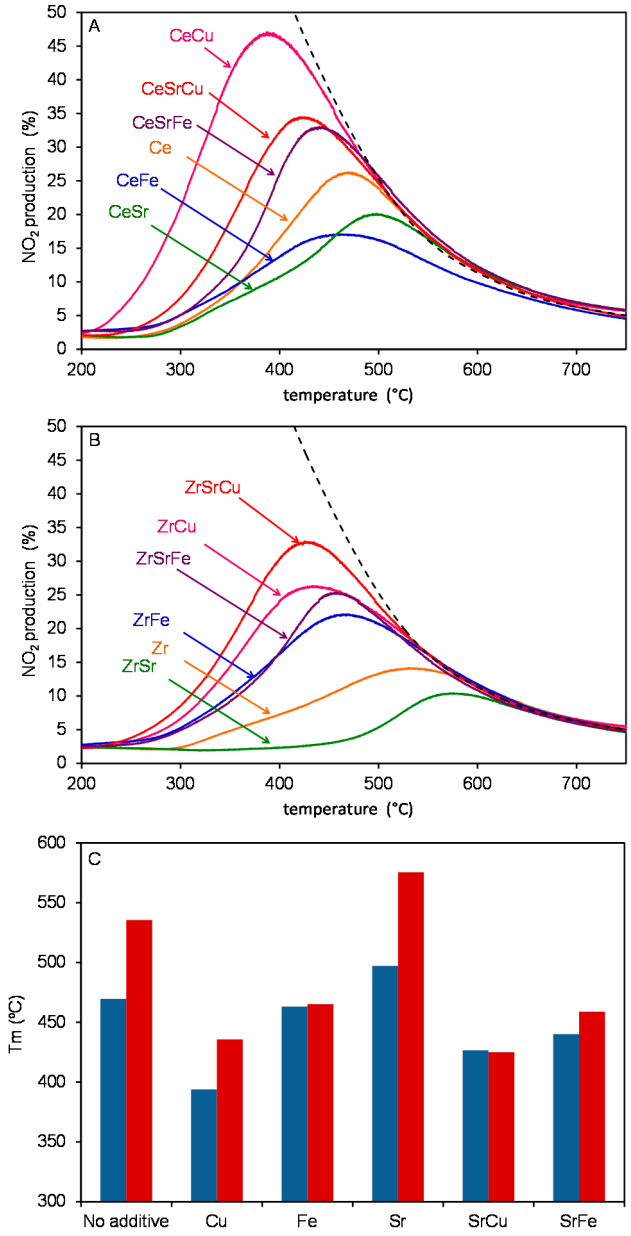

Figure 5. NO_2 production profile for (**A**) Ce- and (**B**) Zr-based catalysts; (**C**) NO oxidation activity: for CeO_2 support (**blue**), ZrO_2 support (**red**).

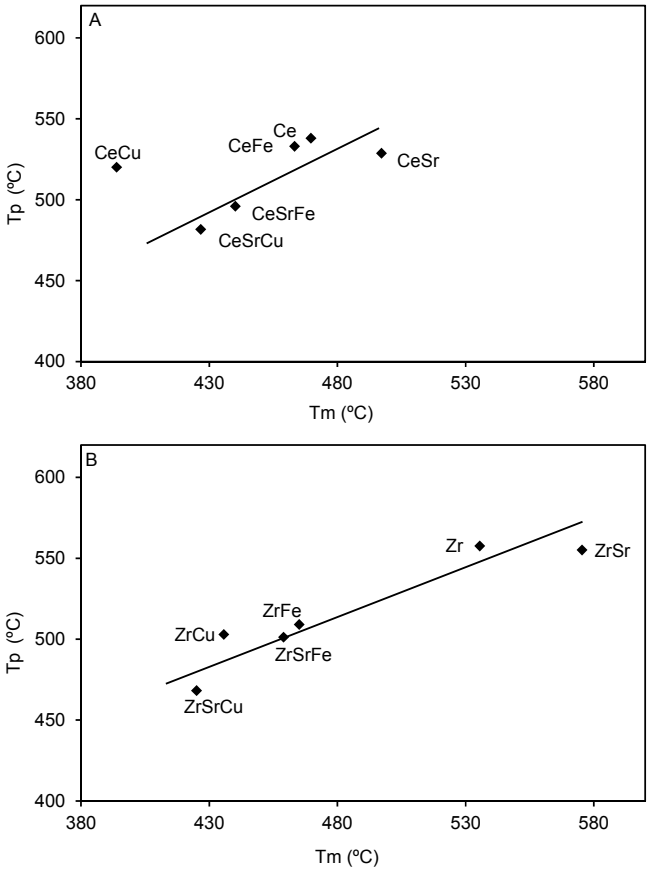

Figure 6. Correlation between *T*p and *T*m for (**A**) Ce- and (**B**) Zr-based catalysts.

With the only exception of CeCu catalyst, Figure 6A shows a tendency of soot oxidation temperature against NO oxidation activity (i.e., the highest is the NO oxidation activity, the highest is the soot combustion temperature). The best catalysts for soot oxidation are the formulations doped with both transition and alkaline-earth metals (in particular CeSrCu and ZrSrCu), which suggests a synergic effect between Cu and Sr, independently from the support. It is well known that, in the presence of NO, alkali-earth metals are mainly involved in the storage of NO_x species [53,54]. Table 2 shows NO_x adsorption/desorption properties obtained from NO_x-TPD experiments.

Table 2. Desorption of NO_x based on NO_x-TPD experiments.

Sample	[a] Desorbed NO_x (μmol/g_{cat})	Sample	Desorbed NO_x (μmol/g_{cat})
Ce	30	Zr	12
CeCu	55	ZrCu	41
CeFe	46	ZrFe	46
CeSr	64	ZrSr	35
CeSrCu	65	ZrSrCu	54
CeSrFe	65	ZrSrFe	63

[a] Amount of NO and NO_2 desorbed in the range of temperature 100–550 °C.

During the NO_x-TPD measurements all of the materials investigated release a significant amount of NO_x species, where the amount released with Ce-based catalysts is higher if compared to Zr-based formulations. The incorporation of Sr further enhances the desorption of NO_x indicating that when Sr is present in the formulation nitrite/nitrate species can be efficiently stored on the sample and then released when increasing the temperature.

To summarize, the transition metal is favourably involved in the oxidation of NO to NO_2, while strontium is involved in the storage of NO_x species. The nitrite/nitrate species stored on strontium, when the temperature increases, start to decompose, releasing NO_x that can easily react with particulate-forming CO and CO_2. At this point, the presence of a transition metal is crucial to recycling NO to NO_2. When Sr is added to the catalyst, the NO_x involved in soot oxidation can originate from the oxidation of NO present in the reaction mixture and from the nitrates stored on the system, positively influencing the particulate combustion activity.

3. Materials and Methods

3.1. Catalyst Preparation

A series of 5 wt % Cu- and Fe-loaded CeO_2 and ZrO_2 doped with 10 wt % of Sr has been prepared according to the following methodology: Supports were synthesized by calcination of cerium nitrates (Treibacher Industrie AG, Althofen, Austria) and zirconium hydroxides (Mel Chemicals, Manchester, UK) at 500 °C for 3 h. After that, aqueous solutions with appropriate amounts of Cu (Copper(II) nitrate hemi (pentahydrate), Sigma Aldrich, Saint Louis, MO, USA), Fe (Iron(III) nitrate nonahydrate, Sigma Aldrich), and/or Sr (strontium nitrate, Strem chemicals, Newburyport, MA, USA) were added by incipient wetness impregnation, and dried overnight at 100 °C. Cu- and Fe-loaded materials were prepared by a single impregnation step, while for catalysts containing Sr, two successive impregnation steps have been applied. After drying the samples were finally calcined at 700 °C for 3 h.

3.2. Catalyst Characterization

Textural characteristics of all fresh samples were measured according to the BET method by nitrogen adsorption at −196 °C, using a Tristar 3000 gas adsorption analyser (Micromeritics, Norcross, GA, USA).

Structural features of the catalysts were characterized by X-ray diffraction (XRD). XRD patterns were recorded on a Philips X'Pert diffractometer (PANalytical B.V., Almelo, The Netherlands) operated at 40 kV and 40 mA with nickel-filtered Cu-Kα radiation. Diffractograms were collected using a step size of 0.02° and a counting time of 40 s per angular abscissa in the range 20–80°. The Philips X'Pert HighScore software (PANalytical B.V., Almelo, The Netherlands, 2002) was used for phase identification. The mean crystalline size was estimated from the full width at the half maximum (FWHM) of the X-ray diffraction peak using the Scherrer equation [73] with a correction for instrument line broadening.

Redox activity was measured by temperature-programmed reduction (TPR) experiments; catalysts (50 mg) were heated at a constant rate (10 °C/min) in a U-shaped quartz reactor from room temperature to 1000 °C under a 4.5% H_2/N_2 flow (35 mL/min). Previously, a pre-treatment was carried out by heating the samples up to 500 °C during 1 h (10 °C/min) in air flow. The hydrogen consumption was monitored using a thermal conductivity detector (TCD) (Autochem II 2920, Micromeritics, Norcross, GA, USA).

The adsorption/desorption of NO_x were investigated by temperature programmed desorption experiments under N_2 after NO_x adsorption at 250 °C. Fifty milligrams of catalyst were exposed for 30 min at 250 °C to a 500 mL/min gas flow with 500 ppm $NO_x/10\%O_2/N_2$. Then, the gas mixture was replaced by pure N_2 and the temperature was cooled down for 30 min. Finally, the desorption experiments were performed in N_2 (500 mL/min) raising the temperature from 100 to 550 °C at 10 °C/min and NO_x species were monitored by a Fourier Transform Infrared Spectroscopy (FT-IR) gas analysers (MultiGas 2030, MKS Instruments, Inc., Andover, MA USA).

3.3. Soot Oxidation Tests

Samples for catalytic measurements were prepared by mixing, in a loose contact condition, known amounts of soot (Printex-U by Degussa) and catalysts, in order to adopt a catalyst/soot weight ratio of 20:1.

Soot oxidation activity was determined from peak-top temperature (*T*p) during temperature programmed oxidation (TPO) of catalyst-soot mixtures. During the TPO measurements 20 mg of mixture were heated at a constant rate (10 °C/min) in a quartz reactor, while the gas flow (10% of O_2/N_2 or 500 ppm NO/10% O_2/N_2) was kept fixed at 500 mL/min. The catalyst temperature was checked by a chromel-alumel thermocouple, located on the catalyst bed.

Outlet composition was monitored by a FT-IR gas analysers (MultiGas 2030, MKS) by recording the percentages of NO, NO_2, CO, and CO_2. Reproducibility of results was verified by running several TPO experiments on similar samples and the results in terms of *T*p were always within 5 °C.

In order to evaluate the NO oxidation capacity of the materials, TPO experiments in a $NO/O_2/N_2$ atmosphere on the as-prepared catalyst were also performed and as a measure of activity the temperature of the maximum production of NO_2 (*T*m) was used.

4. Conclusions

This study focuses on the catalytic behaviour of strontium modified Cu- and Fe-based catalysts in soot oxidation. The addition of Sr positively affected the catalytic activity of the materials, suggesting a synergic effect between transition metals (Cu or Fe) and alkaline-earth metal (Sr). Among all the formulations the most active is CeSrCu; it is proposed that the role of copper is to convert NO into NO_2 following a redox cycle where the copper active sites are alternately oxidized and reduced. The role of strontium seems to be correlated to its ability to store NO_x species and then release NO_x enhancing the NO_x-assisted mechanism. Therefore, this class of materials could be considered as an interesting alternative to Pt-based catalysts for the simultaneous removal of soot and NO_x in LNT applications. Further studies should be performed on their reactivity in the reduction of the stored NO_x.

Acknowledgments: The authors thank financial support from MIUR (Futuro in ricerca, FIRB 2012, project SOLYST) and Regione FVG, through project LR 14/2010.

Author Contributions: E.A. and A.T. conceived and designed the experiments; V.R.-P. and E.A. performed the experiments; V.R.-P. and E.A. analyzed the data; A.T. and E.A. contributed reagents/materials/analysis tools; E.A. wrote the manuscript.

Conflicts of Interest: The authors declare no conflict of interest.

References

1. Neeft, J.P.A.; Makkee, M.; Moulijn, J.A. Diesel particulate emission control. *Fuel Process. Technol.* **1996**, *47*, 1–69. [CrossRef]
2. Summers, J.C.; VanHoutte, S.; Psaras, D. Simultaneous control of particulate and NO_x emissions from diesel engines. *Appl. Catal. B-Environ.* **1996**, *10*, 139–156. [CrossRef]
3. Qian, Z.Q.; Siegmann, K.; Keller, A.; Matter, U.; Scherrer, L.; Siegmann, H.C. Nanoparticle air pollution in major cities and its origin. *Atmos. Environ.* **2000**, *34*, 443–451.
4. Fino, D. Diesel emission control: Catalytic filters for particulate removal. *Sci. Technol. Adv. Mater.* **2007**, *8*, 93–100. [CrossRef]
5. Majewski, W.A.; Khair, M.K. *Diesel Emissions and Their Control*; SAE International: Warrendale, PA, USA, 2006.
6. Twigg, M.V. Controlling automotive exhaust emissions: Successes and underlying science. *Philos. Trans. A Math. Phys. Eng. Sci.* **2005**, *363*, 1013–1033. [CrossRef] [PubMed]
7. Van Setten, B.A.A.L.; Makkee, M.; Moulijn, J.A. Science and technology of catalytic diesel particulate filters. *Catal. Rev.* **2001**, *43*, 489–564. [CrossRef]
8. Van Setten, B.A.A.L.; Schouten, J.M.; Makkee, M.; Moulijn, J.A. Realistic contact for soot with an oxidation catalyst for laboratory studies. *Appl. Catal. B-Environ.* **2000**, *28*, 253–257. [CrossRef]
9. Saracco, G.; Badini, C.; Russo, N.; Specchia, V. Development of catalysts based on pyrovanadates for diesel soot combustion. *Appl. Catal. B-Environ.* **1999**, *21*, 233–242. [CrossRef]
10. Ciambelli, P.; Palma, V.; Russo, P.; Vaccaro, S. Redox properties of a TiO_2 supported Cu-V-K-Cl catalyst in low temperature soot oxidation. *J. Mol. Catal. A-Chem.* **2003**, *204*, 673–681. [CrossRef]

11. Oi-Uchisawa, J.; Obuchi, A.; Enomoto, R.; Xu, J.Y.; Nanba, T.; Liu, S.T.; Kushiyama, S. Oxidation of carbon black over various Pt/MO_x/SiC catalysts. *Appl. Catal. B-Environ.* **2001**, *32*, 257–268. [CrossRef]
12. Hernandez-Gimenez, A.M.; Castello, D.L.; Bueno-Lopez, A. Diesel soot combustion catalysts: Review of active phases. *Chem. Pap.* **2014**, *68*, 1154–1168. [CrossRef]
13. Shimizu, K.; Katagiri, M.; Satokawa, S.; Satsuma, A. Sintering-resistant and self-regenerative properties of Ag/SnO_2 catalyst for soot oxidation. *Appl. Catal. B-Environ.* **2011**, *108*, 39–46. [CrossRef]
14. Aneggi, E.; Llorca, J.; de Leitenburg, C.; Dolcetti, G.; Trovarelli, A. Soot combustion over silver-supported catalysts. *Appl. Catal. B-Environ.* **2009**, *91*, 489–498. [CrossRef]
15. Peralta, M.A.; Zanuttini, M.S.; Querini, C.A. Activity and stability of BaKCo/CeO_2 catalysts for diesel soot oxidation. *Appl. Catal. B-Environ.* **2011**, *110*, 90–98. [CrossRef]
16. Fu, M.L.; Yue, X.H.; Ye, D.Q.; Ouyang, J.H.; Huang, B.C.; Wu, J.H.; Liang, H. Soot oxidation via cuo doped CeO_2 catalysts prepared using coprecipitation and citrate acid complex-combustion synthesis. *Catal. Today* **2010**, *153*, 125–132. [CrossRef]
17. Tikhomirov, K.; Krocher, O.; Elsener, M.; Wokaun, A. MnOx-CeO_2 mixed oxides for the low-temperature oxidation of diesel soot. *Appl. Catal. B-Environ.* **2006**, *64*, 72–78. [CrossRef]
18. Wagloehner, S.; Kureti, S. Modelling of the kinetics of the catalytic soot oxidation on Fe_2O_3. *Appl. Catal. B-Environ.* **2013**, *129*, 501–508. [CrossRef]
19. Reddy, B.M.; Rao, K.N. Copper promoted ceria-zirconia based bimetallic catalysts for low temperature soot oxidation. *Catal. Commun.* **2009**, *10*, 1350–1353. [CrossRef]
20. Gimenez-Manogil, J.; Bueno-Lopez, A.; Garcia-Garcia, A. Preparation, characterisation and testing of CuO/$Ce_{0.8}Zr_{0.2}O_2$ catalysts for NO oxidation to NO_2 and mild temperature diesel soot combustion. *Appl. Catal. B-Environ.* **2014**, *152*, 99–107. [CrossRef]
21. Reichert, D.; Bockhorn, H.; Kureti, S. Study of the reaction of NO_x and soot, on Fe_2O_3 catalyst in excess of O_2. *Appl. Catal. B-Environ.* **2008**, *80*, 248–259. [CrossRef]
22. Aneggi, E.; de Leitenburg, C.; Dolcetti, G.; Trovarelli, A. Promotional effect of rare earths and transition metals in the combustion of diesel soot over CeO_2 and CeO_2-ZrO_2. *Catal. Today* **2006**, *114*, 40–47. [CrossRef]
23. Mei, D.Q.; Yue, S.; Wu, H.; Zhao, X.; Yuan, Y.N. Effect of Co_3O_4 on the kinetics of thermal decomposition of diesel particulate matter. *Emerg. Mater. Res.* **2016**, *5*, 100–109. [CrossRef]
24. Li, H.C.; Li, K.Z.; Wang, H.; Zhu, X.; Wei, Y.G.; Yan, D.X.; Cheng, X.M.; Zhai, K. Soot combustion over $Ce_{1-x}Fe_xO_{2-\delta}$ and CeO_2/Fe_2O_3 catalysts: Roles of solid solution and interfacial interactions in the mixed oxides. *Appl. Surf. Sci.* **2016**, *390*, 513–525. [CrossRef]
25. Liu, S.; Wu, X.D.; Liu, W.; Chen, W.M.; Ran, R.; Li, M.; Weng, D. Soot oxidation over CeO_2 and Ag/CeO_2: Factors determining the catalyst activity and stability during reaction. *J. Catal.* **2016**, *337*, 188–198. [CrossRef]
26. Rico-Perez, V.; Aneggi, E.; Bueno-Lopez, A.; Trovarelli, A. Synergic effect of Cu/$Ce_{0.5}Pr_{0.5}O_{2-\delta}$ and $Ce_{0.5}Pr_{0.5}O_{2-\delta}$ in soot combustion. *Appl. Catal. B-Environ.* **2016**, *197*, 95–104. [CrossRef]
27. Wang, J.G.; Cheng, L.; An, W.; Xu, J.L.; Men, Y. Boosting soot combustion efficiencies over CuO-CeO_2 catalysts with a 3DOM structure. *Catal. Sci. Technol.* **2016**, *6*, 7342–7350. [CrossRef]
28. Aneggi, E.; Leitenburg, C.D.; Trovarelli, A. Ceria-Based Formulations for Catalysts for Diesel Soot Combustion. In *Catalysis by Ceria and Related Materials*, 2nd ed.; Trovarelli, A., Fornasiero, P., Eds.; Imperial College Press: London, UK, 2013; pp. 565–621.
29. Bueno-Lopez, A. Diesel soot combustion ceria catalysts. *Appl. Catal. B-Environ.* **2014**, *146*, 1–11. [CrossRef]
30. Oliveira, C.F.; Garcia, F.A.C.; Araujo, D.R.; Macedo, J.L.; Dias, S.C.L.; Dias, J.A. Effects of preparation and structure of cerium-zirconium mixed oxides on diesel soot catalytic combustion. *Appl. Catal. A-Gen.* **2012**, *413*, 292–300. [CrossRef]
31. Kumar, P.A.; Tanwar, M.D.; Russo, N.; Pirone, R.; Fino, D. Synthesis and catalytic properties of CeO_2 and Co/CeO_2 nanofibres for diesel soot combustion. *Catal. Today* **2012**, *184*, 279–287. [CrossRef]
32. Aneggi, E.; de Leitenburg, C.; Trovarelli, A. On the role of lattice/surface oxygen in ceria-zirconia catalysts for diesel soot combustion. *Catal. Today* **2012**, *181*, 108–115. [CrossRef]
33. Aneggi, E.; Wiater, D.; de Leitenburg, C.; Llorca, J.; Trovarelli, A. Shape-dependent activity of ceria in soot combustion. *ACS Catal.* **2014**, *4*, 172–181. [CrossRef]
34. Aneggi, E.; Divins, N.J.; de Leitenburg, C.; Llorca, J.; Trovarelli, A. The formation of nanodomains of Ce_6O_{11} in ceria catalyzed soot combustion. *J. Catal.* **2014**, *312*, 191–194. [CrossRef]

35. Di Sarli, V.; Landi, G.; Lisi, L.; Saliva, A.; Di Benedetto, A. Catalytic diesel particulate filters with highly dispersed ceria: Effect of the soot-catalyst contact on the regeneration performance. *Appl. Catal. B-Environ.* **2016**, *197*, 116–124. [CrossRef]
36. Andana, T.; Piumetti, M.; Bensaid, S.; Russo, N.; Fino, D.; Pirone, R. Nanostructured ceria-praseodymia catalysts for diesel soot combustion. *Appl. Catal. B-Environ.* **2016**, *197*, 125–137. [CrossRef]
37. Aneggi, E.; de Leitenburg, C.; Dolcetti, G.; Trovarelli, A. Diesel soot combustion activity of ceria promoted with alkali metals. *Catal. Today* **2008**, *136*, 3–10. [CrossRef]
38. Shan, W.J.; Yang, L.H.; Ma, N.; Yang, J.L. Catalytic activity and stability of K/CeO_2 catalysts for diesel soot oxidation. *Chin. J. Catal.* **2012**, *33*, 970–976. [CrossRef]
39. Peralta, M.A.; Zanuttini, M.S.; Ulla, M.A.; Querini, C.A. Diesel soot and NOx abatement on K/La_2O_3 catalyst: Influence of k precursor on soot combustion. *Appl. Catal. A-Gen.* **2011**, *399*, 161–171. [CrossRef]
40. Galvez, M.; Ascaso, S.; Moliner, R.; Lazaro, M. Influence of the alkali promoter on the activity and stability of transition metal (Cu, Co, Fe) based structured catalysts for the simultaneous removal of soot and NO_x. *Top. Catal.* **2013**, *56*, 493–498. [CrossRef]
41. Matarrese, R.; Castoldi, L.; Lietti, L.; Forzatti, P. Soot combustion: Reactivity of alkaline and alkaline earth metal oxides in full contact with soot. *Catal. Today* **2008**, *136*, 11–17. [CrossRef]
42. Russo, N.; Furfori, S.; Fino, D.; Saracco, G.; Specchia, V. Lanthanum cobaltite catalysts for diesel soot combustion. *Appl. Catal. B-Environ.* **2008**, *83*, 85–95. [CrossRef]
43. Fan, G.L.; Zhao, L.; Gong, C.R.; Ma, J.; Xue, G. Effect of supports on soot oxidation of copper catalysts: $BaTiO_3$ versus Fe_2O_3@$BaTiO_3$ core/shell microsphere. *Nano* **2016**, *11*. [CrossRef]
44. Galvez, M.E.; Ascaso, S.; Stelmachowski, P.; Legutko, P.; Kotarba, A.; Moliner, R.; Lazaro, M.J. Influence of the surface potassium species in Fe-K/Al_2O_3 catalysts on the soot oxidation activity in the presence of nox. *Appl. Catal. B-Environ.* **2014**, *152*, 88–98. [CrossRef]
45. Laversin, H.; Courcot, D.; Zhilinskaya, E.A.; Cousin, R.; Aboukais, A. Study of active species of Cu-K/ZrO_2 catalysts involved in the oxidation of soot. *J. Catal.* **2006**, *241*, 456–464. [CrossRef]
46. Lick, I.D.; Carrascull, A.L.; Ponzi, M.I.; Ponzi, E.N. Zirconia-supported Cu-KNO_3 catalyst: Characterization and catalytic behavior in the catalytic combustion of soot with a NO/O_2 mixture. *Ind. Eng. Chem. Res.* **2008**, *47*, 3834–3839. [CrossRef]
47. Wu, X.D.; Liang, Q.; Weng, D.; Lu, Z.X. The catalytic activity of CuO-CeO_2 mixed oxides for diesel soot oxidation with a NO/O_2 mixture. *Catal. Commun.* **2007**, *8*, 2110–2114. [CrossRef]
48. Wagloehner, S.; Kureti, S. Study on the mechanism of the oxidation of soot on Fe_2O_3 catalyst. *Appl. Catal. B-Environ.* **2012**, *125*, 158–165. [CrossRef]
49. Lopez-Suarez, F.E.; Bueno-Lopez, A.; Illan-Gomez, M.J.; Adamski, A.; Ura, B.; Trawczynski, J. Copper catalysts for soot oxidation: Alumina versus perovskite supports. *Environ. Sci. Technol.* **2008**, *42*, 7670–7675. [CrossRef] [PubMed]
50. Soler, L.; Casanovas, A.; Escudero, C.; Perez-Dieste, V.; Aneggi, E.; Trovarelli, A.; Llorca, J. Ambient pressure photoemission spectroscopy reveals the mechanism of carbon soot oxidation in ceria-based catalysts. *Chemcatchem* **2016**, *8*, 2748–2751. [CrossRef]
51. Milt, V.G.; Querini, C.A.; Miro, E.E.; Ulla, M.A. Abatement of diesel exhaust pollutants: NOx adsorption on Co,Ba,K/ CeO_2 catalysts. *J. Catal.* **2003**, *220*, 424–432. [CrossRef]
52. Pisarello, M.L.; Milt, V.; Peralta, M.A.; Querini, C.A.; Miro, E.E. Simultaneous removal of soot and nitrogen oxides from diesel engine exhausts. *Catal. Today* **2002**, *75*, 465–470. [CrossRef]
53. Matarrese, R.; Castoldi, L.; Lietti, L.; Forzatti, P. Simultaneous removal of NO_x and soot over Pt-Ba/Al_2O_3 and Pt-K/Al_2O_3 DPRN catalysts. *Top. Catal.* **2009**, *52*, 2041–2046. [CrossRef]
54. Lin, F.; Wu, X.D.; Weng, D. Effect of barium loading on CuO_x-CeO_2 catalysts: NO_x storage capacity, NO oxidation ability and soot oxidation activity. *Catal. Today* **2011**, *175*, 124–132. [CrossRef]
55. Weng, D.A.; Li, J.; Wu, X.D.; Si, Z.C. NO_x-assisted soot oxidation over K/CuCe catalyst. *J. Rare Earth* **2010**, *28*, 542–546. [CrossRef]
56. Fierro, J.L.G. *Metal Oxides: Chemistry and Applications*; CRC Press: Boca Raton, FL, USA, 2005.
57. Castoldi, L.; Aneggi, E.; Matarrese, R.; Bonzi, R.; Llorca, J.; Trovarelli, A.; Lietti, L. Silver-based catalytic materials for the simultaneous removal of soot and NO_x. *Catal. Today* **2015**, *258*, 11. [CrossRef]
58. Shen, Q.; Lu, G.Z.; Du, C.H.; Guo, Y.; Wang, Y.Q.; Guo, Y.L.; Gong, X.Q. Role and reduction of NO_x in the catalytic combustion of soot over iron-ceria mixed oxide catalyst. *Chem. Eng. J.* **2013**, *218*, 164–172. [CrossRef]

59. Martinez-Arias, A.; Gamarra, D.; Fernandez-Garcia, M.; Hornes, A.; Bera, P.; Koppany, Z.; Schay, Z. Redox-catalytic correlations in oxidised copper-ceria CO-PROX catalysts. *Catal. Today* **2009**, *143*, 211–217. [CrossRef]
60. Li, G.S.; Smith, R.L.; Inomata, H. Synthesis of nanoscale $Ce_{1-x}Fe_xO_2$ solid solutions via a low-temperature approach. *J. Am. Chem. Soc.* **2001**, *123*, 11091–11092. [CrossRef] [PubMed]
61. Wang, H.; Qu, Z.P.; Xie, H.B.; Maeda, N.; Miao, L.; Wang, Z. Insight into the mesoporous $Fe_xCe_{1-x}O_{2-\delta}$ catalysts for selective catalytic reduction of NO with NH_3: Regulable structure and activity. *J. Catal.* **2016**, *338*, 56–67. [CrossRef]
62. Giordano, F.; Trovarelli, A.; de Leitenburg, C.; Giona, M. A model for the temperature-programmed reduction of low and high surface area ceria. *J. Catal.* **2000**, *193*, 273–282. [CrossRef]
63. Magnacca, G.; Cerrato, G.; Morterra, C.; Signoretto, M.; Somma, F.; Pinna, F. Structural and surface characterization of pure and sulfated iron oxides. *Chem. Mater.* **2003**, *15*, 675–687. [CrossRef]
64. Soni, K.C.; Shekar, S.C.; Singh, B.; Gopi, T. Catalytic activity of Fe/ZrO_2 nanoparticles for dimethyl sulfide oxidation. *J. Colloid Interface Sci.* **2015**, *446*, 226–236. [CrossRef] [PubMed]
65. Pojanavaraphan, C.; Luengnaruemitchai, A.; Gulari, E. Effect of support composition and metal loading on Au catalyst activity in steam reforming of methanol. *Int. J. Hydrogen Energ.* **2012**, *37*, 14072–14084. [CrossRef]
66. Sang, X.L.; Li, K.Z.; Wang, H.; Wei, Y.G. Selective oxidation of methane and carbon deposition over $Fe_2O_3/Ce_{1-x}Zr_xO_2$ oxides. *Rare Met.* **2014**, *33*, 230–238. [CrossRef]
67. Tang, X.L.; Zhang, B.C.; Li, Y.; Xu, Y.D.; Xin, Q.; Shen, W.J. CuO/CeO_2 catalysts: Redox features and catalytic behaviors. *Appl. Catal. A-Gen.* **2005**, *288*, 116–125. [CrossRef]
68. Arango-Diaz, A.; Cecilia, J.A.; Moretti, E.; Talon, A.; Nunez, P.; Marrero-Jerez, J.; Jimenez-Jimenez, J.; Jimenez-Lopez, A.; Rodriguez-Castellon, E. Comparative study of CuO supported on CeO_2, $Ce_{0.8}Zr_{0.2}O_2$ and $Ce_{0.8}Al_{0.2}O_2$ based catalysts in the CO-PROX reaction. *Int. J. Hydrogen Energ.* **2014**, *39*, 4102–4108. [CrossRef]
69. Zabilskiy, M.; Djinović, P.; Tchernychova, E.; Tkachenko, O.P.; Kustov, L.M.; Pintar, A. Nanoshaped Cuo/CeO_2 materials: Effect of the exposed ceria surfaces on catalytic activity in N_2O decomposition reaction. *ACS Catal.* **2015**, *5*, 5357–5365. [CrossRef]
70. Muroyama, H.; Hano, S.; Matsui, T.; Eguchi, K. Catalytic soot combustion over CeO_2-based oxides. *Catal. Today* **2010**, *153*, 133–135. [CrossRef]
71. Kustov, A.L.; Makkee, M. Application of NO_x storage/release materials based on alkali-earth oxides supported on Al_2O_3 for high-temperature diesel soot oxidation. *Appl. Catal. B-Environ.* **2009**, *88*, 263–271. [CrossRef]
72. Kustov, A.L.; Ricciardi, F.; Makkee, M. NO_x storage and high temperature soot oxidation on $Pt\text{-}Sr/ZrO_2$ catalyst. *Top. Catal.* **2009**, *52*, 2058–2062. [CrossRef]
73. Jenkins, R.; Snyder, R. *Introduction to X-ray Powder Diffractometry*; Wiley: New York, NY, USA, 1996.